ACCURACY ENHANCEMENT OF TERRESTRIAL MOBILE LIDAR DATA USING THEORY OF ASSIMILATION

H. Yousif [a, *], J. Li [a], M. Chapman [b], Y. Shu [a]

[a] University of Waterloo, Dept. of Geography, 200 University Avenue W., Waterloo, Canada, N2L 3G1
(hyousif, jli, y2shu)@uwaterloo.ca
[b] Dept. of Civil Engineering, Ryerson University, Victoria St., Toronto, Canada M5B 2K1 - mchapman@ryerson.ca

Commission VI, WG VI/4

KEY WORDS: LiDAR, Terrestrial MMS, Geo-referencing, Data assimilation, Chi-squared

ABSTRACT:

Even though the terrestrial LiDAR mobile mapping system is fairly new, it has been rapidly ingested by end users of wide spectrum of disciplines. As more and more applications are enjoying the potential of terrestrial LiDAR systems, refining quality and accuracy of LiDAR data is becoming increasingly critical. While the average geo-referencing accuracy of terrestrial LiDAR systems currently reaches the decimetre level under good GPS conditions, further post geo-referencing enhancement still need to be explored to make up for accuracy deterioration under all conditions. Alternatively, users may seek costly solutions such as building ground control stations to overcome this problem. Furthermore, the radiometric intensity is yet another important aspect that needs to be addressed. This paper discusses the feasibility of using the theory of data assimilation in enhancing positioning and radiometric intensity. Two terrestrial LiDAR datasets of the same area were integrated using assimilation method. The resulted model produced better accuracy as indicated by the comparison to a reference shapefile as well as the standard deviations. A Chi-squared test was also performed where the hypothesis of the estimated value is accepted as the true state at the 95% and 99% confidence level for 3D coordinates whereas it is rejected for the intensity.

1. INTRODUCTION

The concept of Terrestrial Mobile Mapping Systems (MMS) has started to materialize into actual development over the last decade of the previous century. The first research prototypes were launched concurrently at the Department of Geomatics Engineering at University of Calgary (El-Sheimy, 1996) and the Centre of Mapping at Ohio State University (Bossler and Toth, 1996) which resulted into development of two optical mobile mapping systems namely, VISAT by University of Calgary and GPSVan™ by Ohio State University. In 2000, the Institut Cartogràfic de Catalunya (ICC), based in Barcelona, developed a camera-based terrestrial MMS known as GEOVAN which was capable of acquiring and geo-referenced digital images (Talaya et al., 2004a). Earlier systems involved indirect geo-referencing by employing exterior orientation elements and existing ground control stations (Tao and Li, 2007). However, the incorporation of the Light Detection And Ranging (LiDAR) sensors into those terrestrial mobile mapping systems for ranging and profiling purposes had to wait for several years before it could become viable; and persisted to remain out of the picture even after the implication of LiDAR sensors into the Airborne-based systems for large scale topographic mapping (Toth, 2009a). The reason for that is, perhaps, most of the surveying commercial corporations, which operate on local scales, cannot afford the high cost of those systems. On the other hand, stationary LiDAR systems such as laser rangefinders and profilers have been commonly used during the last 30 years for traditional surveying measurements. Those systems are integrated with total stations for highly accurate measurements of individual points in land surveying. Nevertheless, those measurements were not sufficient when topographic surveys were demanded for large scale area. Such needs motivated the development of terrestrial static LiDAR systems which were used later for automated measurements of thousands of points in the field surrounding the sensor within a short period of time. They are equipped with a laser rangefinder and a mirror that is automatically rotated by a horizontal and vertical encoder. The range measurements are recorded simultaneously with the angular measurements whose horizontal and vertical pitches are programmed to change at equal increments in order to obtain an equally spaced spatial sampling (Shan and Toth, 2008). Neither static LiDAR sensors nor total stations support direct geo-referencing as they are not provided with GPS/IMU system. With the advent of the new integrated technologies of GPS and Inertial Navigation Systems (INS) during the nineties, the MMS has experienced significant improvements that facilitated the procedures of direct geo-referencing rather than relying on prearranged control points. Further, when the GPS constellation became fully operational and selective availability was disengaged, the direct geo-referencing processes were able to achieve remarkably higher positioning accuracies. In addition, the switch from analogue to digital electronics systems has reflected positively in the processes of data acquisition, storing and analysis. Within the last few years, the term of MMS has been used interchangeably with MMT that refers to the Mobile Mapping Technology, which indicates the soaring reliance of MMS on recent technology (Schwartz and El-Sheimy, 2007). Eventually, those technological advances paved the way for the début of the terrestrial LiDAR mobile mapping systems which become of a particular importance as more and more geospatial applications, such as city modeling and web GIS, solicit high demands of 3D accurate visualization. Moreover, the terrestrial

* Corresponding author

LiDAR mobile mapping systems are exigently needed to satisfy the requirements of emergency and disaster management which calls for accurate, relevant and on-time geospatial information.

One of the earliest research efforts of developing a terrestrial LiDAR MMS was the Vehicle-borne Laser Mapping System (VLMS) which was handled by the Centre for Spatial Information Science at the University of Tokyo in 2001 (Shan and Toth, 2008). In 2003, the Institut Cartogràfic de Catalunya (ICC) successfully integrated and operated LiDAR sensors into GEOMOBIL system which is the modified version of the aforementioned camera-based GEOVAN MMS (Talaya et al., 2004b). The Finnish Geodetic Institute has been developing a Vehicle-borne LiDAR system known as ROAMER since 2003 (Kukko et al., 2007). In contrast, the business-oriented Geomatics companies such as Optech Inc. (Canada), Terrapoint Inc. (Canada) and 3D Laser Mapping (UK) were not standing aloof from that forum where they have been providing terrestrial LiDAR MMS services of highway surveys (Zampa et al., 2009; Jaakkola et al., 2008), urban area 3D reconstruction modeling (Zampa et al., 2009), fluvio-estuarine monitoring (Hetherington et al., 2007) and scanning coastal environment (Barber et al., 2007). Only since 2006 have some of those service providers started to sell their proprietary terrestrial LiDAR MMS products on the wake of the growing demand.

Compared to photogrammetric MMS, LiDAR MMS enjoy several advantages which render the former MMS as a secondary system. Some of those features include its nature as an active system that enables LiDAR MMS to operate at day and night, as well as its capability of direct geo-referencing without the need of triangulation or orthorectification.

In this paper, an optimization algorithm which is based on the theory of assimilation is developed to improve the accuracy of both positioning and radiometric data.

2. DIRECT GEO-REFERENCING OF LIDAR POINT CLOUD

Direct geo-referencing is defined as the process of determining the time-variable spatial position of a point (or points) scanned by a mobile mapping sensor with reference to a local or a global coordinate system. In order to accurately geo-reference the scanned point, it is necessary to determine the 3D instantaneous coordinates of the center of mass of the LiDAR sensor with reference to the mapping frame (i.e. the local or a global coordinate system). The 3D coordinates of the sensor's center of mass is a time varying function that depends on the observed measurements of the sensor's position and orientation. At present, the integrated GPS/INS system is the key component in both terrestrial and airborne LiDAR mapping sensors, which is responsible for taking the position and orientation measurements. While the GPS system provides the position and velocity at a typical measurement rate of 1 Hz, the INS measures the roll, yaw and pitch which describe the orientation of the vehicle at around 100,000 Hz measurement rate. The INS is also capable of computing the accurate position and velocity, thus filling the gap between GPS measurements or during GPS outages. The GPS, in turn, continually fixes the drift error of the INS (Shan and Toth, 2008).

It has to be noted that the GPS will not be able to directly measure the instantaneous 3D coordinates of the sensor's center of mass, nor – as a result – the 3D coordinates of the scanned point, as it can only measure the position of the GPS antenna. However, the INS can accurately measure the attitude of both the sensor's center of mass and the GPS antenna which are located at fixed known offsets from the INS. The INS consists of three gyroscopes and three accelerometer for measuring the 3D angular velocity and acceleration respectively (Shan and Toth, 2008). It is, therefore, necessary to apply the principles of kinematic modeling and vector mathematics to compute the 3D position of the scanned point at any instant of time, with the INS taken as the hub of computation for the reasons mentioned above. Figure 2 below illustrates the coordinate systems of the various components of the terrestrial LiDAR MMS and a point object (*P*). The direct geo-referencing procedure involves a few transformations between the different coordinate systems of which the rotation matrices are well defined. The mapping frame can be chosen as the geodetic control system (longitude, latitude and height), Universal Transverse Mercator System (UTM) or any other Earth Centered Earth Fixed (ECEF) coordinate system.

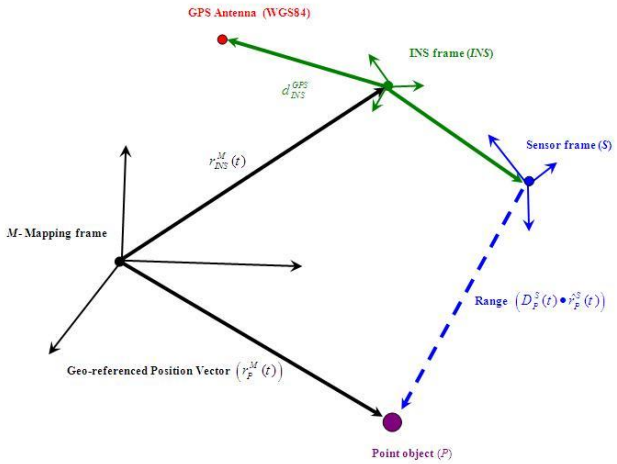

Figure 1. Direct Geo-referencing components

From the above figure, the instantaneous position vector $r_P^M(t)$ of the mapped point *P* as referenced to the mapping frame *M* is given by the following equation (Barber et al., 2008):

$$r_P^M(t) = r_{INS}^M(t) + R_{INS}^M(t) \bullet \left(d_S^{INS} + R_S^{INS} \bullet D_P^S(t) \bullet \hat{r}_P^S(t) \right) \quad (1)$$

which represents the resultant vector of the sum of three vectors $r_{INS}^M(t)$, d_S^{INS} and $D_P^S(t) \bullet \hat{r}_P^S(t)$, where

$r_P^M(t)$ is the instantaneous position vector of the object point with reference to the mapping *M*- frame

$r_{INS}^M(t)$ is the instantaneous position vector of the IMU with reference to the mapping *M*- frame

$R_{INS}^M(t)$ is the instantaneous rotation matrix from the *INS*-frame to the *M*- frame

d_S^{INS} is the constant offset vector between the IMU and Sensor's centre of mass with reference to the *INS*-frame

R_S^{INS} is the constant rotation matrix from the *S*-frame to the *INS*- frame

$D_P^S(t)$ instantaneous scalar distance measured by the LiDAR sensor as a range from the object point

$\hat{r}_P^S(t)$ is the instantaneous unit vector between the point P and the sensor's centre

Note that the geo-referenced vector $r_{INS}^M(t)$ of the IMU itself can be expressed as:

$$r_{INS}^M(t) = r_{GPS}^M(t) - R_{INS}^M(t) \bullet d_{GPS}^{INS} \quad (2)$$

where:

$r_{GPS}^M(t)$ is the instantaneous position vector of the GPS antenna with reference to the mapping *M*- frame

d_{GPS}^{INS} is constant offset vector between the IMU and GPS antenna

3. RESEARCH PROBLEM

The cloud point data provided by a LiDAR sensor, which consists of mainly geo-referenced 3D positional and radiometric information, is utilized to service many details-oriented applications including 3D building reconstruction models, monitoring of urban infrastructure and feature extraction of road environment. The accuracy of such data is of a critical importance for those applications as it largely determines the quality of the produced information. In addition, the accuracy of positional information is the major trait of LiDAR point cloud that distinguishes it from photogrammetric data. Accurate height information, for instance, facilitated kerbstones detection in a road surface modeling study conducted by Jaakkola et al. (2008) using terrestrial LiDAR data. In another example, the StreetMapper system is frequently used by Cambridgeshire Traffic Police in UK to scan the crash debris along with the surrounding road environment, in the event of serious accidents, within short period of time (Hunter et al., 2006).

To obtain a reliable direct geo-referencing, the raw measurements from the IMU and GPS receiver are subjected to complex operations which include double integrals of the 3D acceleration as well as the differential GPS (DGPS) processing (Shan and Toth., 2008). The DGPS helps computing the various GPS errors originating from atmospheric absorption, satellite and receiver clock drifts and receiver hardware as well as performing ambiguity resolutions by combining simultaneous data from two receivers (Hoffmann-Wellenhof et al., 2008). The inertial state vector values resulting from that integral are susceptible to error propagations; therefore, Kalman filtering is used to continuously update those values. GPS receivers, on the other hand, are occasionally prone to GPS signal outage due to signal obstruction by buildings or trees which results in cycle slips that leads to incorrect positioning calculations. Conversely, the INS will be able to fix the incorrect GPS calculations by detecting and correcting those short term cycle slips. Implementing such rigorous procedures by some of LiDAR systems manufacturers in their current terrestrial LiDAR MMS resulted in high quality of positioning accuracies that range from 3 cm for StreetMapper (Hunter et al., 2006), 5 cm for LYNX (Optech, 2009) and 10 cm for FGI ROAMER (FGI, 2009). Unfortunately, achieving those accuracies is bound to clear sky conditions or buildings-free area, and only within certain proximity from the mapped object. The positioning accuracy of GEOMOBIL was found to degrade from 30 cm at a distance of 20 m from the object to 1 m at only 40 m from the object (Alamus et al., 2005). The accuracy of GPS measurements may also suffer due to multipath effect as the vehicle passes through urban areas, which is an inevitable scenario, where multiple signals are reflected from nearby buildings. In built area, the StreetMapper accuracy was found to drop to 50 cm (Hunter et al., 2006).

From the foregoing discussion, it can be concluded that LiDAR point cloud may not always produce the desired accuracy unless additional remedies are applied within or after data acquisition. Hetherington et al. (2007) had to build an independent GPS control network of static stations to augment the accuracy of estuarine environment representation using terrestrial LiDAR MMS. In a highway survey between Korinthos and Athens in Greece using LYNX, Zampa et al. (2009) set up six base stations and a number of ground control points at intervals of 50 – 80 m along the 60 km highway road. While the point cloud accuracy for that survey was improved to 1 – 2 cm level, the associated overhead cost may defeat the defense of using terrestrial LiDAR MMS as a cost effective solution. LYNX was used, as well, to develop a 3D reconstruction model of a historical area in Leicester city (UK). Owing to the high buildings and corridors, the GPS signal was often interrupted by outage and multipath which necessitated the incorporation of a Distance Measurement Indicator (DMI) in the system to fix drift errors during outages (Zampa et al., 2009). Figure 2 below shows DMI which is a wheel-mounted instrument that precisely measures the traveled distance. DMI was also used by Alamus et al. (2005) during the investigation of ICC's GEOMOBIL performance.

Figure 2. Distance Measurement Indicator (Zampa et al., 2009)

As opposed to photogrammetric data, LiDAR point cloud has yet another drawback pertaining to its ability of presenting semantic and topological information. While potential investigations have been targeting positional, orientation and range deliverables of LiDAR point clouds, extremely little effort, if any, is done to address LiDAR radiometric intensity. To the best knowledge of the author, there is not even a single method that shows how systems manufacturers are calibrating LiDAR intensity. Perhaps a compelling reason for that is the huge volume of LiDAR point cloud which only makes it worse to add any image attributes. To make up for that shortcoming, researchers often resort to fusion of LiDAR point cloud with optical imagery. Terrapoint Inc. developed an integrated system that adds scan colour capability to the LiDAR sensor (Mrstik et al., 2009). Fusion with optical imagery have gone even further to temporarily replace GPS, as demonstrated by Toth et al. (2009b) who proposed an alternative navigation tool to provide real time positioning information during GPS outages using existing terrain optical data.

4. DATASET

The dataset consists of terrestrial LiDAR point cloud over a 1700 m closed loop at Espoonlahti neighborhood in Espoo, about 15 km west of Helsinki. The data extent covers five road

segments of Espoonlahdenkatu, Espoonlahdentie, Merenkulkijankatu, Kipparinkatu and Espoonlahdenranta streets in addition to Lippulaiva shopping mall. The point cloud was collected by the vehicle-based FGI ROAMER at a measurement frequency of 48 Hz in two opposite directions. The data was made available to researchers for free through the FGI ftp server.

5. METHODOLOGY

This paper uses a statistically-based algorithm that aims at refining the positional and radiometric accuracies of LiDAR point cloud. This algorithm utilizes the theory of data assimilation to enhance the 3D geo-referencing accuracy as well as fine-tuning the radiometric intensity by means of exploiting the correlation between two oppositely-collected datasets over the same study area. For this approaches, it is assumed that the mapped object will exhibit consistent response to the LiDAR sensor regardless of the direction of motion as depicted by

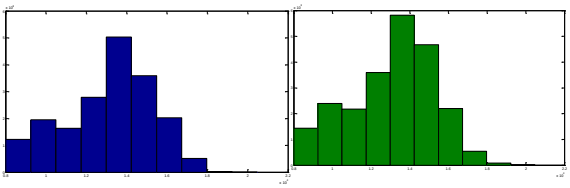

Figure 3. Histograms of radiometric intensity for both trips

5.1 Theory of Assimilation

Data assimilation is an optimization algorithm that is based on the principle of least squares analysis. The purpose of data assimilation is to combine two different datasets or models of the same phenomenon in order to achieve the best estimate of the true state. This method was proved to be viable by Reichle (2008) who used it to integrate satellite remotely sensed snow data with ground field hydrology measurements. Having found this method to be successful for the case of snow data which were collected by two different systems over different scales, the LiDAR case will, presumably, has much higher probability of success as it was collected by the same LiDAR sensor over the same area and scale under the same ambient conditions. Even more, the two LiDAR datasets were collected over relatively same period of time unlike the case of snow data. Apparently, therefore, data assimilation will have better chances of recognizing the underlying correlation between the two LiDAR datasets. Those factors, altogether, are the rationale behind choosing data assimilation to enhance the accuracy of LiDAR data.

Suppose that we have two different datasets V_i and V_j of a certain phenomenon. Let σ_i^2 and σ_j^2 be their respective variances. Now if V is the true state, then our goal to minimize the weighted sum of squared residuals:

$$J = w_i \left(V_i - V\right)^2 + w_j \left(V_j - V\right)^2 = \frac{\left(V_i - V\right)^2}{\sigma_i^2} + \frac{\left(V_j - V\right)^2}{\sigma_j^2} \quad (3)$$

where

J is known as the cost function and w_i , w_j are the weights

The best estimate $\hat{V}$ can be obtained by differentiating equation (3) and equating the derivative to zero, which yields:

$$\hat{V} = \left(\sigma_j^2 + \sigma_i^2\right)^{-1} \left(\sigma_j^2 V_i + \sigma_i^2 V_j\right) \quad (4)$$

It might be of interest to demonstrate the robustness of this model by computing the variance of $\hat{V}$:

$$\mathrm{var}(\hat{V}) = \frac{\sigma_i^2 \sigma_j^2}{\sigma_j^2 + \sigma_i^2} < \sigma_i^2 \ or \ \sigma_j^2 \quad (5)$$

which implies that the new model is closer to the true state than either dataset.

In the event of having multivariable dataset, equation (4) can be generalized as follows:

$$\hat{V} = inv\left(\mathrm{cov}(V_i) + \mathrm{cov}(V_j)\right) * \left(\mathrm{cov}(V_j) * V_i + \mathrm{cov}(V_i) * V_j\right) \quad (6)$$

5.2 Assimilation of LiDAR point clouds

As mentioned previously, the assimilation process uses the existing correlation between different observations of a particular phenomenon in order to obtain the best estimate of the true state.

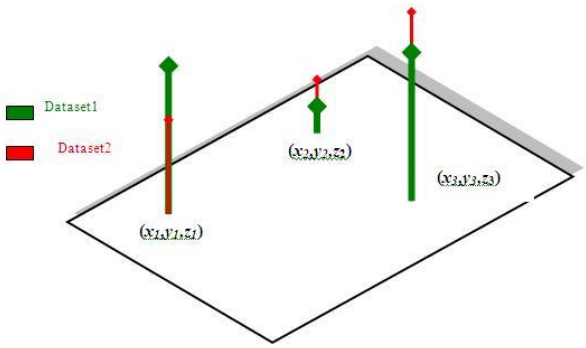

Figure 4. Assimilation of two datasets

The assimilation method is meant to integrate the attributes of two datasets that are corresponding to the same geospatial positions as shown in Figure 4 where the two datasets occupy the same 3D coordinates. However, in the case of LiDAR data, the geospatial positions themselves, in addition to the intensity, need to be assimilated. Since the 3D coordinates of the two LiDAR point clouds do not coincide (they will coincide only if they are both true state), a new definition should be introduced to decide on which points are to be assimilated.

The LiDAR point cloud is irregularly spaced by nature, which will be inherited when the two datasets are blended. The criterion of which points are to be assimilated should be based on the spatial neighbourhood. When the two datasets are merged, points from one dataset might come closer to other points of the second dataset, and then only the points that are sufficiently close will be assimilated. The status of *sufficiently close* will be declared for those points that are closer than the minimum spacing of each point cloud individually. If point A

and point B (Figure 5) are two points from the forward and reversed data cloud then they will be assimilated if:
AB < minimum spacing of point cloud A AND minimum spacing of point cloud B

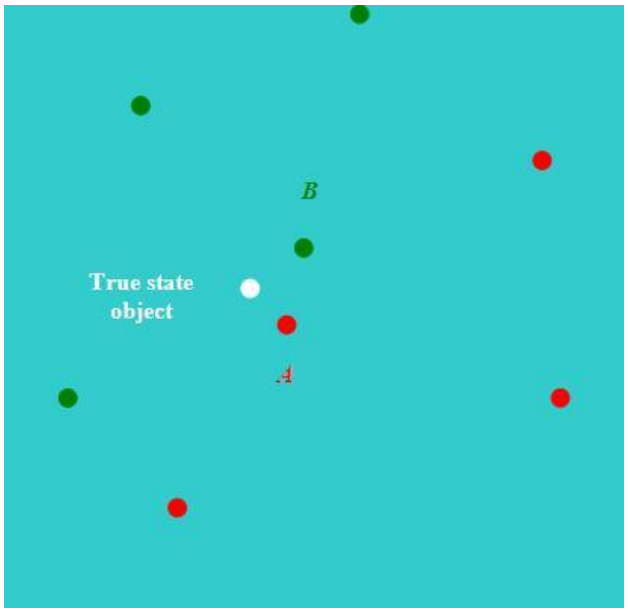

Figure 5. Assimilation Criterion

When that status occurs, the laser sensor is, most likely, targeting the same object (labeled as white), yet missing the exact position because of error measurements. The new point that results from assimilating *A* and *B* will me more accurate and closer to the true state as indicated by equation (5). However, there is a subtle downside for this approach as it suggests replacing two points with only one point which reduces the resolution of the LiDAR point cloud when it is least expected to improve it. This situation can be avoided by changing the AND in the criterion to OR:
AB < minimum spacing of point cloud A OR minimum spacing of point cloud B
The following cases will be encountered during processing when *A* and *B* are sufficiently close:

Case (I): The spacing between *A* and *B* is less than the minimum spacing of the first point cloud and greater than that of the second point cloud. In this case *A* will be replaced with the assimilated point while *B* is retained. No point is lost.

Case (II): This is just the opposite of Case (I). Again, no point is lost.

Case (III): The spacing between A and B is less than the minimum spacing of both the first point cloud and the second point cloud. In this case both *A* and *B* will be replaced with the assimilated point. To avoid reducing the resolution we can include the assimilated point as well as retaining *A* or *B*, whichever is closer to the assimilated point.

Having done that, the total number of points will be exactly equal to the sum of the individual datasets. Provided that the average spacing of the LiDAR point cloud of this research is 5 cm and the minimum spacing is around 1 cm, the positioning accuracy is expected to be within cm level.

6. RESULTS

A subset of two oppositely collected datasets is examined for the purpose of this research. The selected datasets contains of mainly building, vegetation and road environment. Each dataset consists of around 75,000 points. Figure 8 illustrates the forward and reverse point cloud before merging.

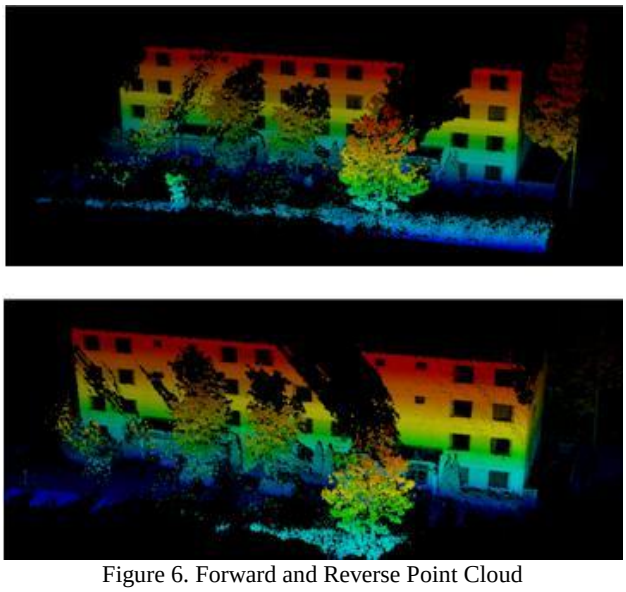

Figure 6. Forward and Reverse Point Cloud

The two point clouds were firstly merged without assimilation. Then the assimilation was performed on the merged data. Figure 7 shows the merged and assimilated results. For both cases produces better visibility than the individual datasets.

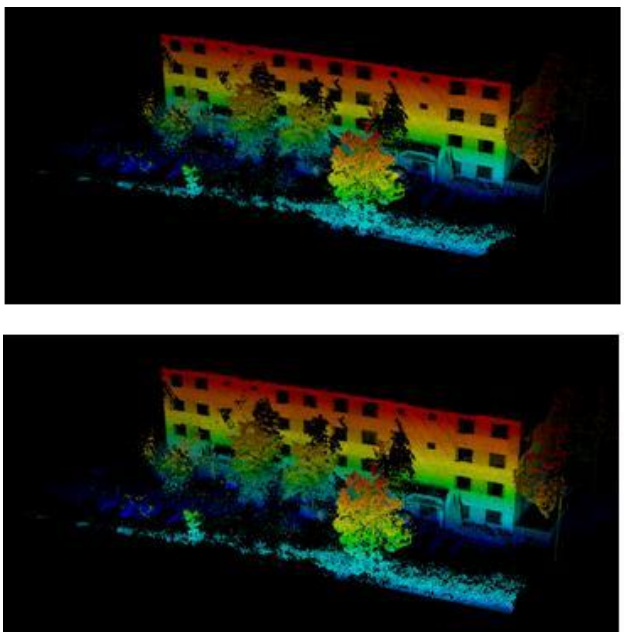

Figure 7. Simple merged result (top) and Assimilated result (bottom)

Even though the assimilated and merged results shows no difference in terms of visibility, the assimilated results produced better accuracy as indicated by Table 1.

	X (cm)	Y (cm)	Z (cm)	Intensity
Forward dataset	3.26	0.03	2.55	39.37
Reverse dataset	2.88	0.03	2.63	42.41
Simple merging	1.97	0.03	2.46	38.92
Assimilated model	1.77	0.02	2.44	37.03

Table 1. Comparisons between standard deviations of different components

Validation

Two validation methods were applied for this research. The first one is comparing the results to a reference shapefile and the second one is testing the null hypothesis of $V = \hat{V}$ using Chi-squared distribution.

Reference Shapefile

A 5 cm buffer zone was built over the reference shapefile of a building at the study area. The total number of points within that buffer zone was found to be 38,941 points for the simple merged result versus 74,851 points for the assimilated result which was almost doubled as illustrated by Figure 8. Recalling that no interpolation was carried out for this research, the only explanation for that density increase in case of assimilated model is that more points came closer to the true state.

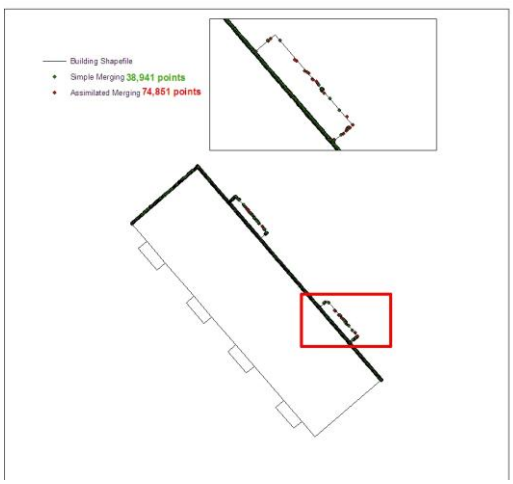

Figure 8. 5cm Buffer zone around the reference shapefile

Chi-squared Test

The following expression was computed using the observed data and the assimilated model as the expected value for each of three coordinates and the intensity:

$$\sum \left[\frac{\left(E - O_{forward}\right)^2}{E} + \frac{\left(E - O_{reverse}\right)^2}{E} \right]$$

The result is shown in Table 2 below:

	X	Y	Z	Intensity
χ^2 value	4.7e-6	1.8e-7	0.0169	1775.5

Table 2. Chi squared values

The failure of accepting the hypothesis for case of intensity signifies that the assimilation of intensity should not be treated the same way as the 3D coordinates. One of the reasons that the hypothesis test fails, is that the intensity is mistakenly assumed as having the same correlation as the position. This assumption is evidently erroneous especially when one considers two adjacent points of different classes such as asphalt and ground or building and vegetation where the intensity changes remarkably while the position is still correlated. This problem can be resolved by setting a threshold for difference between intensity values beyond which the intensity should not be assimilated.

Conclusion

This paper presented an optimization algorithm that aimed at enhancing the quality of LiDAR data pertaining to geo-referencing and radiometric intensity. The theory of data assimilation was used to combine two terrestrial LiDAR datasets that were collected in two opposite directions over the same area. The assimilated model was compared to the observed data as well as a simple merged model. A reference shapefile and standard deviations was used for validation. The result demonstrated that the assimilated model produced better accuracy. A Chi-square test was carried out to the test the hypothesis that the assimilated model equals the true state at 95% and 99% confidence level. It was shown that the estimated values of 3D coordinates can be accepted as true state while it is rejected for the intensity.

References

Alamus, R., A. Baron, J. Casacuberta, M. Pla, S. Sànchez, A. Serra, and J. Talaya, 2005, GEOMOBIL: ICC Land-based Mobile Mapping System for Cartographic Data Capture, *Proceedings 22nd International Cartographic Conference, Corunna, Spain, 9 pp*

Barber, D. M., J. Mills, and S. Smith-Voysey, 2008. Geometric Validation of a Ground-Based Mobile Laser Scanning System, *ISPRS Journal of Photogrammetry & Remote Sensing* **63 (2008)**, 128–141

Barber, D. M., and J. P. Mills, 2007. Vehicle Based Waveform Laser Scanning in a Coastal Environment, *5th International Symposium on Mobile Mapping Technologies*

Bossler, J. D., and C. K. Toth, 1996. Feature Positioning Accuracy in Mobile Mapping: Results Obtained by the GPSVan™, *International Archives of Photogrammetry and Remote Sensing*, ISPRS Comm. IV, **Vol. 31, Part B4**: pp. 139-142.

El-Sheimy, N., 1996. The Development of VISAT – A Mobile Survey System for GIS Applications, (PhD Thesis), *UCGE Report No. 20101, Department of Geomatics Engineering, University of Calgary*

Finnish Geodetic Institutte (FGI), 2009. Espoonlahti LiDAR point cloud data and description, retrieved from ftp.fgi.fi, last accessed on July 1st, 2009

Hetherington D., S. German, M. Utteridge, D. Cannon, N. Chisholm and T. Tegzes, 2007. Accurately Representing a Complex Estuarine Environment Using Terrestrial LiDAR, *RSPoc Conference, September 2007, Newcastle Upon Tyne, UK*

Hoffmann-Wellenhof, B., H. Lichtengger, and E. Wasle, 2008. *GNSS – Global Positioning Satellite Systems: GPS, GLONASS, Galileo and more*, SpringerWeinNewYork , 2008

Hunter, G., C. Cox, and J. Kremer, 2006. Development of a Commercial Laser Scanning Mobile Mapping System - StreetMapper, *Second International Workshop, The Future of Remote Sensing, Antwerp, Belgium, October 17-18, 2006, 4 pp*

Jaakkola, A., J. Hyyppä, H. Hyyppä, and A. Kukko, 2008. Retrieval Algorithms for Road Surface Modeling Using Laser-Based Mobile Mapping, *Sensors* **2008**, 8, 5238-5249; DOI: 10.3390/s8095238

Kukko, A., C. O. Andrei, V. M. Salminen, H. Kaartinen, Y. Chen, P. Ronnholm, H. Hyyppä, J. Hyyppä, R. Chen, H. Haggren, I. Kosonen and K. Capek, 2007. Road environment mapping system of the Finnish Geodetic Institute - FGI ROAMER**,** *International Archives of Photogrammetry, Remote Sensing and Spatial Information Sciences*, 36(3/W52), 241-247

Mrstik, P., and K. Kusevic, 2009. Real Time 3D Fusion of Imagery and Mobile LiDAR, *ASPRS 2009 Annual Conference, Baltimore, Maryland, March 9-13, 2009*

Optech Inc., 2009. LYNX Mobile Mapper, retrieved from http://www.optech.ca/pdf/LynxDataSheet.pdf, last accessed on December 10th, 2009

Reichle, R. H., 2008. Data assimilation Methods in the Earth sciences, *Advances in Water Resources*, **Vol. 31**, Issue 11, 1411-1418

Schwarz, K.P. and N. El-Sheimy, 2007. *Digital Mobile Mapping Systems – State-of-the-Art and Future Trends, Advances in Mobile Mapping Technology*, Eds. Tao and Li, Taylor & Francis Group, pp. 3-18.

Shan, J. and C. K. Toth, Eds., 2008. *Topographic Laser Ranging And Scanning – Principles and Processing*, CRC Press, Taylor & Francis Group

Talaya, J., Bosch, E., Alamus, R., Serra, A., and Baron, A., 2004a, Geovan: The Mobile Mapping System from the ICC. *Proceedings of the 4th International symposium on Mobile Mapping Technology, Kunming, China, March 29-31,2004, 7 pp.*

Talaya, J., Alamus, R., Bosch, E., Serra, A., Kornus, W., and Baron, A., 2004b, Integration of Terrestrial Laser Scanner with GPS/IMU Orientation Sensors. *International Archives of Photogrammetry and Remote Sensing, ISPRS Comm. V*, **Vol. 35**, Part B5, 6 pp.

Tao, V., and J. Li, Eds., 2007. *Advances in Mobile Mapping Technology*, Taylor & Francis Group, London, UK

Toth, C. K., 2009a. R&D of Mobile LiDAR Mapping and Future Trends, *ASPRS 2009 Annual Conference, Baltimore, Maryland, March 9-13, 2009*

Toth, C. K., D. A. Grejner-Brzezinska, J. N. Markiel, 2009b. Terrain-Based Navigation: A Tool to Improve Navigation and Feature Extraction Performance of Mobile Mapping Systems, *6th International Symposium on Mobile Mapping Technology, Sao Paulo, Brazil, July 21-24, 2009*

Zampa, F., and D. Conforti, 2009. Mapping with Mobile LiDAR, *GIM International*, **Vol. 23**, Issue 4, pages 35-37